Consolidation of Partially Stabilized ZrO_{2} in the Presence of a Noncontacting Electric Field

Hasti Majidi and Klaus van Benthem

Consolidation of partially stabilized ZrO_2 in the presence of a non-contacting electric field

Hasti Majidi and Klaus van Benthem[*]

Department of Chemical Engineering and Materials Science, University of California, Davis, CA, 95616, USA

*Corresponding author. Email:benthem@ucdavis.edu. Ph: +1 530 7525117

Abstract

Electric field-assisted sintering techniques have demonstrated accelerated densification at lower temperatures than the conventional sintering methods. However, it is still debated whether the applied field and/or resulting currents are responsible for the densification enhancement. To distinguish the effects of an applied field from current flow, *in situ* scanning transmission electron microscopy experiments with soft agglomerates of partially stabilized yttria-doped zirconia particles were carried out. A new micro-electromechanical system-based sample support was used to heat particle agglomerates while simultaneously exposing them to an externally applied non-contacting electric field. Under isothermal condition at 900°C, an electric field strength of 500 V/cm shows a sudden three-fold enhancement in shrinkage of agglomerates. The applied electrostatic potential lowers the activation energy for point defect formation within the space charge zone and therefore promotes consolidation. Obtaining similar magnitudes of shrinkage in the absence of any electric field requires higher temperature and longer time.

Keywords: *In situ* STEM, electric field-assisted sintering, YSZ, TEM, image processing, shrinkage

Sintering describes the formation of fully-dense polycrystalline microstructures from loose powder agglomerates typically by applying high temperatures and mechanical pressure. [1–3] Electric field-assisted sintering (EFAS) techniques, including spark plasma sintering [4–7] and "flash sintering" [8–10] have demonstrated accelerated densification and lower sintering temperatures compared to conventional sintering in the absence of any applied electric field or current. It is still under debate, however, whether the applied electric field, the resulting current through the sample, or both are responsible for the accelerated sintering. [11] While the current flow throughout the sample could enhance densification through suggested mechanisms such as electromigration, [12,13] Joule heating, [14,15] and self-cleaning [16,17] at grain boundaries, it is proposed that the electric field could enhance sintering by nucleation of point defects, [18,19] dielectric breakdown of insulating surface layers, [20,21] and interactions with space charge layers [18,22].

The objective of this work was to investigate how non-contacting electric fields in the absence of any electrical current affect consolidation of softly-agglomerated 3 mol% yttria-stablized ZrO_2 (3YSZ). *In situ* transmission electron microscopy (TEM) enables direct observation of particles during exposure to externally applied stress fields, and can, therefore, provide mechanistic information about the consolidation process. Several previous studies report neck formation and growth between two coalescing particles, which is representative of the initial stage of sintering. [23–25] More recently, Holland *et al*. have investigated two nickel particles brought into contact with each other using a scanning tunneling microscopy tip inside the TEM. Neck formation and growth, relative particle rearrangement and eventual coalescence

was observed as a result of an applied electrical bias that lead to current flow through the contacting particles. [15] Subsequently, Bonifacio *et al*. have shown that dielectric breakdown of insulating surface oxide layers can cause a retardation for current-assisted consolidation, and was recognized as a dominant mechanism for previously observed surface cleaning effects. [16,20] Unlike for the two-particle configuration, consolidation of larger particle agglomerates also includes information about pore evolution that is essential to be considered for sintering studies. In a recent publication we have reported *in situ* TEM sintering experiments of 3YSZ particle agglomerates and proposed techniques to derive quantitative densification plots representing the microstructural evolution of the particle agglomerates during heat treatment. [26]

A mechanistic description of EFAS techniques requires the separation of electrical current and electric field effects on the powder agglomerates. Here, we demonstrate the use of a micro-electromechanical system (MEMS) device during *in situ* scanning transmission electron microscopy (STEM) experiments that, for the first time, enables application of homogeneous electric fields on powder agglomerates without exposing electrical current to the sample. *In situ* STEM imaging was used to monitor the microstructural evolution of the agglomerates during isothermal densification with and without exposure to an applied electrical field. The acquired micrographs were subsequently used to generate densification curves for a quantitative analysis of shrinkage as a function of time and applied electrical field strength.

3YSZ nanoparticles (TOSOH USA, TZ-3Y-E) with an average diameter of 40 nm were dispersed in ethanol and then drop-casted onto MEMS devices (Protochips, Inc.) capable of both heating and biasing. Figure 1 shows schematics of the electro-thermal MEMS device with an agglomerate supported by electron-transparent amorphous carbon (a-carbon) which covers a holey membrane of SiC serving as a resistive heating element. [27,28] The non-contacting

electric field is formed by biasing two parallel 100-nm thick W electrodes, deposited on a 50-nm thick Si_3N_4 layer. Si_3N_4 interlayer is necessary to minimize current leakage to the heating membrane. The distance between the electrodes inducing the field is at least two orders of magnitude larger than the size of agglomerates; hence, the applied electric field is considered homogeneous. Two separate power supplies are used to supply the heating current and the electrical bias for heating in the presence of non-contacting electrical field, respectively. The heating currents are calibrated up to 900 °C to avoid potential inconsistencies in the morphology and resistance of W electrodes at higher temperatures. For an electrical field strength of 500 V/cm at 900 °C, the experimentally observed leakage current resulting from the bias applied to the W electrodes was at least 3-6 orders of magnitude smaller than the current applied for resistive heating of the SiC membrane. Therefore, the applied bias to generate the electrical field did not contribute to any additional heating of the powder agglomerates. A comparison between the heating current and the measured current resulting from applied field at different temperatures is provided in the supplemental information. [29] In between individual image acquisitions, the electron beam was blocked from irradiating the sample in order to avoid beam-induced modifications of the powder agglomerates.
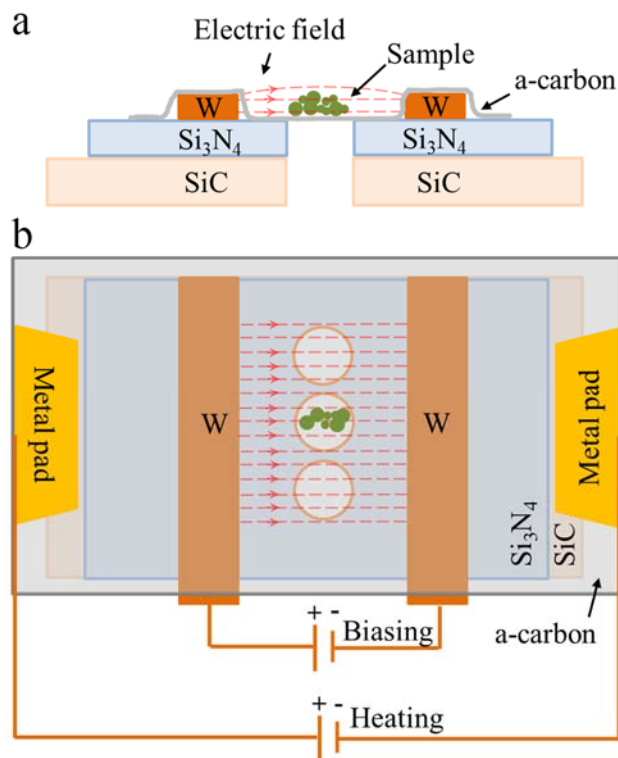
Figure 1: (color online) a) side-view and b) top-view schematics of a Protochips electro-thermal MEMS device. Particle agglomerates, supported by a-carbon, are heated by resistive heating of the underlying SiC membrane. Electric biasing of two parallel W electrodes by a separate power supply generates a homogenous non-contacting electric field across the 3YSZ agglomerates.

In situ STEM observations enable monitoring the morphological evolution and shrinkage of agglomerates during consolidation. Figure 2 shows a series of transient annular dark field (ADF) STEM images of 3YSZ agglomerates recorded with no externally applied electric field (Figure 2(a-e)), and when exposed to an electrical field strength of 500 V/cm (Figure 2(f-h)). In the absence of any electrical field, the temperature was initially raised to 900 °C within 100 s (Figure 2(b-c)), subsequently increased to 1000 °C (Figure 2(d)), and, finally further increased to 1200 °C (Figure 2(e)). For the experiments in the presence of an electric field, instantaneous heating to 900 °C was applied with simultaneous biasing to obtain a field strength of 500 V/cm. Control experiments have revealed no significant morphological changes of the particle

agglomerates for different heating rates. The electrothermal devices used to apply non-contacting electrical fields (see Figure 1) do not allow heating above 900 °C. Therefore, the temperature was held constant at 900 °C for the duration of the experiment in the presence of the applied electric field.

Morphological changes of 3YSZ agglomerates at 900 °C in the absence of any applied electric field are insignificant even after 106 min. However, the agglomerate subjected to an electric field strength of 500 V/cm clearly reveals particle coalescence and pore shrinkage after only 4 min at 900 °C. Dotted rectangles in Figure 2(a-e) mark a specific region within the agglomerate to track particle coalescence during *in situ* consolidation in the absence of an applied field. In Figure 2(a-b) the marked area reveals negligible changes in particle sizes immediately after heating to 900 °C. However, coalescence of particles is observed from the same area at 1000 °C and above (Figure 2(d-e)). The arrows in Figure 2(a-c) point out two small pores whose sizes remain almost unchanged after heating for 106 min at 900 °C. The same pores are shrunk after consecutive heating at 1000 °C for 28 min (Figure 2(d)), and are almost completely closed when the temperature is raised to 1200 °C for 1 min (Figure 2(e)). We have previously shown that the onset temperature for consolidation of 3YSZ agglomerates during *in situ* TEM is around 960 °C. [26] Therefore, no significant changes in morphology of the agglomerate was expected at 900 °C. However, when the agglomerate is exposed to an electric field strength of 500 V/cm, shrinkage of the agglomerate is noticeable after only 4 minutes (see Figure 2(f-h)). The insets in Figure 2(f-h) confirm inter-particle neck growth and particle coalescence in the presence of the electrical field. In addition, the arrows in Figure 2(f-h) mark two pores that shrink and eventually close. Interestingly, grain sizes and their distribution as well

as faceting of individual grains remain unchanged irrespective of whether an electrical field was

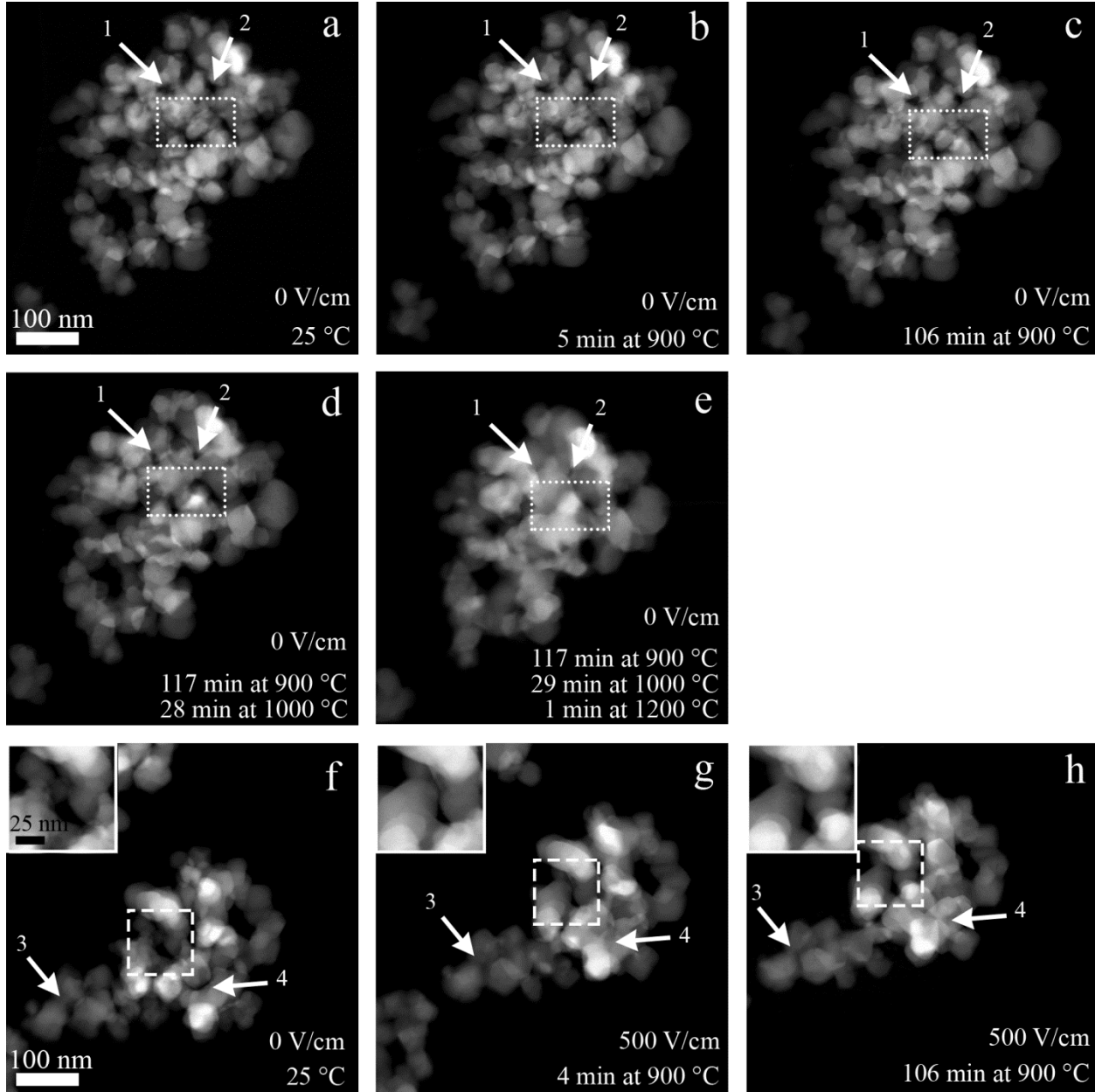applied during *in situ* heating experiments.

Figure 2: STEM micrographs of 3YSZ agglomerates during *in situ* sintering in the absence (a-e) and presence (f-h) of non-contacting electric field. Heating the agglomerate at 900 °C for (b) 4 min and (c) 106 min does not show substantial morphological change of the agglomerate. However, subsequent elevation of temperature to (d) 1000 °C for 28 min and (e) 1200 °C for 1 min shows particle coalescence and pore shrinkage, hence indicating densification (compare dotted rectangles). When agglomerates are subjected to heating at 900 °C and an electric field

strength of 500 V/cm, significant morphological changes are observed (g-h). The insets in (f-h) are magnified version of areas marked by dashed rectangles, and show neck growth, particle coalescence and pore closure when an electric field is applied.

In order to quantitatively analyze densification during *in situ* consolidation and investigate the effect of an applied electric field on shrinkage of agglomerates, image processing was used to track the projected area of the agglomerates obtained from the recorded STEM micrographs. [26]   The projected area of the agglomerate that includes internal pores is subsequently labeled *filled area*, and was normalized to the initial agglomerate size at 25 °C (time = 0). Similar to our previous work, we assume that shrinkage of filled area reflects volume shrinkage. [26]   Figure 3 shows the normalized filled area of the two agglomerates shown in Figure 2 during *in situ* densification without and with electric field as a function of time. The experimental error bar considers the accuracy of focusing during image acquisition and is approximately 1%. At 900 °C, the normalized filled area of the agglomerate in the absence of the electric field decreases slowly to 97% after 106 min. The agglomerate shrinks with a faster rate upon heating at 1000 °C. The normalized filled area reaches 94% after additional heating at 1000 °C for 28 min. Heating of the agglomerate to 1200 °C causes further shrinkage to roughly 82%. However, at this temperature the carbon support film ruptures because of exerted stress by the shrinking agglomerate, which makes determination of relative shrinkage inaccurate. Hence, the filled area pertaining to the agglomerate at 1200 °C (see Figure 2(e)) was not included in Figure 3. While rupturing of the support membrane induces uncertainties to the projected area, the morphological features of the agglomerate at 1200 °C, i.e., size and uniformity of the grains can still be evaluated for a comparison to that of the agglomerate at lower temperatures. When an electric field strength of 500 V/cm is applied during *in situ* densification of the agglomerate at

900 °C, the normalized filled area sharply reduces to 93% of its original value after only 4 min. Figure 3 indicates that obtaining similar amounts of shrinkage without an applied field requires significantly longer time and higher temperature (117 min at 900 °C and 28 min at 1000 °C). Additional experimental data have revealed that applied electric fields can reduce required temperatures by up to 100°C to obtain similar amounts of shrinkage compared to those observed in the absence of any applied fields (see supplemental online materials). The observation of accelerated shrinkage in the presence of externally applied non-contacting electric fields was found to be independent of agglomerate size, i.e., number of agglomerated particles.

The electric field affects shrinkage, i.e., densification immediately when it is applied, and remains almost ineffective as heating and biasing continues. Figure 3 demonstrates that in the presence of the electric fields the agglomerate undergoes initial shrinkage by approximately 7% while its size reduces by only an additional 2% as the experiment proceeds. Moreover, the difference in the normalized filled area of the agglomerate with and without field is approximately 5%. The magnitude of shrinkage observed in this study is significantly smaller compared to those reported for macroscopic flash sintering experiments carried out at much lower electric field strengths. [8] However, during flash sintering electrodes inducing the electric field have direct contact with the sample and allow current flow. Francis *et al* [19] report a direct relationship between sample shrinkage and applied current density, while an increased applied electric field shortens the incubation time for flash sintering as a function of temperature. In this study, a non-contacting electrical field was used in order to disable current flow through the sample. Francis and co-workers postulated that the applied electric field creates a high concentration of defects within the material that can increase both mass transport and electrical conductivity. [19] This description is consistent with dielectric breakdown phenomena that

ultimately lead to local leakage currents [20] and thus, current assisted densification [11,30,31]. It must be noted, however, that conduction mechanisms in 3YSZ are strongly temperature dependent and can involve both ionic and electronic currents. The experimental results presented in this study demonstrate that an applied electric field in the absence of any current flow can affect the densification behavior. Enhanced mass transport observed in this study is a result of defect formation between two adjacent powder particles. The externally applied electric field E lowers the electrochemical potential of vacancies ΔG_f in the space-charge zone [32] following $\Delta G_f = \Delta G_0 + Ze\Phi_i - Ze\Phi_a$. ΔG_0 is Gibbs' free energy of the standard state, Z the charge on the respective ion, e the electron charge, and Φ_i is the internal electrical potential. $\Phi_a = E\lambda$ represents the externally applied electric potential generating a field strength E. λ is the total width of the space charge layer, i.e., twice the Debye length. The reduced electrochemical potential within the space charge zone corresponds to smaller formation energies for point defects. Following the above equation, an electric field applied to powder agglomerates will therefore accelerate defect formation at constant temperature and promotes materials transport through diffusion to the interparticle contacts, i.e. neck formation. Defect formation is further promoted by theoretically predicted field amplification at interparticle contacts [33]. Local defect generation and their percolation is a precursor for subsequent dielectric breakdown of the ceramic if current flow was permitted. Results obtained by flash sintering experiments [19] are consistent with this interpretation. Further investigations such as spatially resolved chemical analysis across forming necks and grain boundaries are required to monitor the formation of defects as a function of applied field. However, such experiments are beyond the scope of this study.
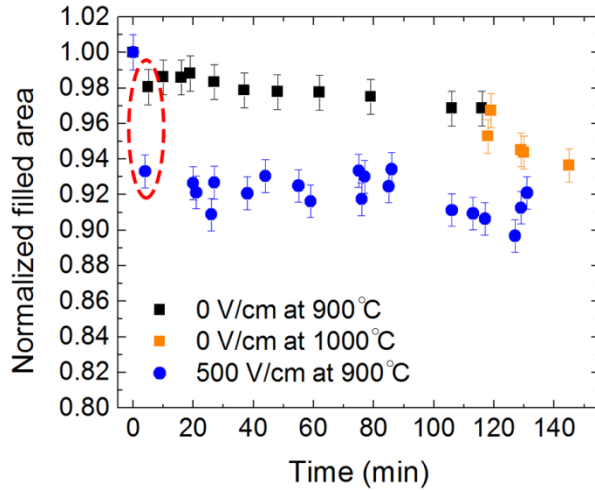
Figure 3: (color online) Normalized filled area of 3YSZ agglomerates in the absence (squares) and presence of an electric field strength of 500 V/cm (circles). Both experiments were performed isothermally at 900 °C (dark squares and circles). The agglomerate was additionally heated to 1000 °C when no field was applied (light squares).

In conclusion, this study reports *in situ* STEM experiments that have demonstrated that applied electric fields in the absence of any current flow can accelerate consolidation of 3YSZ powder agglomerates. Electric fields were applied to individual soft particle agglomerates inside the TEM using a new MEMS-based sample support that enables simultaneous heating and exposure to electric fields during *in situ* STEM imaging. At 900°C, 3YSZ agglomerates only shrink about 3% after 116 min. However, for an applied field strength of 500V/cm a sudden morphological change including neck formation and growth, particle coalescence and pore shrinkage was observed. The microstructural changes led to 7% agglomerate shrinkage immediately after field application. The applied electrostatic potential lowers the activation energy for point defect formation within the space charge zone and, hence, promotes neck formation and consolidation. The experimental results demonstrate that applied electric fields in the absence of any current can accelerate the sintering processes. The observed enhancement in

consolidation induced by the non-contacting electric field is small compared to current-assisted densification of a macroscopic sample, e.g., under flash sintering conditions. Hence, enhanced defect formation as identified indirectly through the quantitative microstructural characterization suggests that dielectric breakdown is necessary for accelerated consolidation of dielectric ceramics.

Acknowledgments

References

[1]   R. M. German, *Sintering Theory and Practice* (John Wiley & Sons, Inc., 1996).

[2]   S. Kang, *Sintering: Densification, Grain Growth and Microstructure* (Elsevier Butterworth-Heinemann, New York, 2004).

[3]   G. L. Messing and A. J. Stevenson, Science. **322**, 383 (2008).

[4]   E. A. Olevsky, S. Kandukuri, and L. Froyen, J. Appl. Phys. **102**, 114913 (2007).

[5]   U. Anselmi-Tamburini, J. E. Garay, Z. A. Munir, A. Tacca, F. Maglia, and G. Spinolo, J. Mater. Res. **19**, 3255 (2011).

[6]   D. Yang, R. Raj, and H. Conrad, J. Am. Ceram. Soc. **93**, 2935 (2010).

[7]   D. Yang and H. Conrad, Scr. Mater. **63**, 328 (2010).

[8]   M. Cologna, B. Rashkova, and R. Raj, J. Am. Ceram. Soc. **93**, 3556 (2010).

[9]   M. Cologna, A. L. G. Prette, and R. Raj, J. Am. Ceram. Soc. **94**, 316 (2011).

[10]   A. Uehashi, K. Sasaki, T. Tokunaga, H. Yoshida, and T. Yamamoto, Microscopy **63**, i19 (2014).

[11]   J. E. Garay, Annu. Rev. Mater. Res. **40**, 445 (2010).

[12]   I. A. Blech and C. Herring, Appl. Phys. Lett. **29**, 131 (1976).

[13]   J. E. Garay, S. C. Glade, U. Anselmi-Tamburini, P. Asoka-Kumar, and Z. A. Munir, Appl. Phys. Lett. **85**, 573 (2004).

[14]   J. Narayan, Scr. Mater. **69**, 107 (2013).

[15]   T. B. Holland, A. M. Thron, C. S. Bonifacio, A. K. Mukherjee, and K. van Benthem, Appl. Phys. Lett. **96**, 243106 (2010).

[16]   J. R. Groza and A. Zavaliangos, Mater. Sci. Eng. A **287**, 171 (2000).

[17]   C. S. Bonifacio, T. B. Holland, and K. Van Benthem, Scr. Mater. **69**, 769 (2013).

[18]   R. Raj, M. Cologna, and J. Francis, J. Am. Ceram. Soc. **7**, 1941 (2011).

[19]   J. S. C. Francis and R. Raj, J. Am. Ceram. Soc. **96**, 2754 (2013).

[20]   C. S. Bonifacio, J. F. Rufner, T. B. Holland, and K. van Benthem, Appl. Phys. Lett. **101**, 093107 (2012).

[21]   R. Chaim, Mater. Sci. Eng. A **443**, 25 (2007).

[22]   J.-W. Jeong, J.-H. Han, and D.-Y. Kim, J. Am. Ceram. Soc. **83**, 915 (2004).

[23]   J. Rankin and L. A. Boatner, J. Am. Ceram. Soc. **77**, 1987 (1994).

[24]   J. Rankin and B. Sheldon, Mater. Sci. Eng. A **204**, 48 (1995).

[25]   M. A. Asoro, D. Kovar, Y. Shao-Horn, L. F. Allard, and P. J. Ferreira, Nanotechnology **21**, 025701 (2010).

[26]   H. Majidi, T. Holland, and K. van Benthem, Ultramicroscopy **152**, 35 (2015).

[27]   J. Damiano, D. Nackashi, and S. Mick, Microsc. Microanal. **14**, 1332 (2008).

[28]   L. F. Allard, W. C. Bigelow, M. Jose-Yacaman, D. P. Nackashi, J. Damiano, and S. E. Mick, Microsc. Res. Tech. **72**, 208 (2009).

[29]   See Supplemental Material [url], which includes Refs. [34-35]

[30]   R. Baraki, S. Schwarz, and O. Guillon, J. Am. Ceram. Soc. **95**, 75 (2012).

[31]   J. E. Garay, S. C. Glade, U. Anselmi-Tamburini, P. Asoka-Kumar, and Z. A. Munir, Appl. Phys. Lett. **85**, 573 (2004).

[32]   H. Conrad and D. Yang, Philos. Mag. **90**, 1141 (2010).

[33]   T. B. Holland, U. Anselmi-Tamburini, D. V. Quach, T. B. Tran, and A. K. Mukherjee, J. Eur. Ceram. Soc. **32**, 3659 (2012).

[34]   S. Heiroth, T. Lippert, A. Wokaun, Appl. phys. A **93**, 639 (2008).

[35]   Y. Pauleau, P. B. Barna, *Protective coatings and thin films: synthesis, characterization and applications* (Springer, 1997).